

The contour of cementless femoral stem has minor effect on initial periprosthetic von Mises stress distribution

A 3-dimensional finite element analysis

Kong-Zu Hu, MD, Xian-Long Zhang, MD, PHD, Cheng-Tao Wang, PHD, Wen-Ting Ji, PHD.

ABSTRACT

الأهداف: تقييم توزيع الجهد مع التكلسات الاسمنتية للجدوع الفخذية من مختلف الجهات.

الطريقة: أجريت هذه الدراسة بقسم العظام – مستشفى شانقهاي السادس – مدينة شانقهاي – الصين، ما بين الفترة مايو 2008م حتى فبراير 2009م. تم تركيب نماذج من عنصر الفينيت للطرف الفخذي القريب مع أربعة جذوع من التكلسات الاسمنتية (الوكلاسيك، ريبب التشرحي، فيرسي، وسيكروي). تحت ظروف التحميل من المشي وصعود الدرج، تم حساب ثلاثة من توزيع الجهد القياسي، وتمت مقارنة نماذج التوزيع.

النتائج: ازداد الجهد في المستوى الأول والثاني والثالث تحت حالتى التحميل الاثنتين وأكثر اعتباراً في المستوى الثاني والثالث. كان الجهد أعلى في الجانب الوسطي في جميع الحالات. لم يتم ملاحظة فرقاً في النماذج بين الجذوع الأربعة.

خاتمة: لدى تصميم الجذع الفخذي تأثير بسيط على توزيع الجهد.

Objectives: To evaluate periprosthetic von Mises stress distribution with cementless femoral stems of various contours.

Methods: The study was carried out at the Department of Orthopaedics, Shanghai 6th Hospital, Shanghai, China between May 2008 and February 2009. Finite element models of proximal femoral replacement with 4 cementless stems (Alloclassic, Ribbed Anatomic, VerSys, and Securi-fit) of various contours were set up. Under the loading conditions of walking and stair climbing, 3-dimensional periprosthetic von Mises stresses were calculated, and the stress distribution patterns were compared.

Results: Periprosthetic stresses were increased in level 1, 2, and 3 under the 2 loading conditions, and

more considerably in level 2 and 3. The stresses were higher on the medial side in all cases. No remarkable difference was found in the patterns between the 4 stems.

Conclusion: The contour design of femoral stem has minor effect on initial periprosthetic von Mises stress distribution.

Saudi Med J 2009; Vol. 30 (7): 947-951

From the Department of Orthopaedic Surgery, the 6th Shanghai People's Hospital, Shanghai Jiaotong University school of Medicine (Hu, Zhang), and the Institute of Biomedical Manufacturing and Life Quality Engineering (Wang, Ji), Shanghai Jiaotong University, Shanghai, PR China.

Received 9th March 2009 Accepted 13th May 2009.

Address correspondence and reprint request to: Dr. Xian-Long Zhang, Department of Orthopaedic Surgery, the 6th Shanghai People's Hospital, Shanghai Jiaotong University School of Medicine, Shanghai, PR China. Tel. +86 5900688376. E-mail: hukongzu@yahoo.com.cn

To avoid “cement disease”, cementless femoral stems have been widely used, especially for younger and more active cases.¹ Current cementless hip replacement is among successful surgery to improve end-stage hip arthrosis.² However, there are usually some cases needing revisions because of failure. The causes of failure are multiple: fracture, infection, dislocation, loosening, and so forth.³ Aseptic loosening is the main reason of failure for hip arthroplasty. Significant periprosthetic bone loss follows hip arthroplasty in the proximal femur.^{4,5} As the magnitude of bone loss is essential to loosening and

Disclosure. No commercial relationship was involved in this work. This study was supported by the Chinese National Natural Science Foundation, Grant No. 30470455.

hence to long-term survivorship of the prosthesis, many efforts have been made to improve it. Among the causes of bone loss, the effect of stress shielding is a major one for both cemented and cementless femoral stems. Due to the intrinsic bigger profile, cementless stems are more vulnerable in terms of stress shielding. Proximal stress distribution has been demonstrated to be closely correlated with bone loss. Therefore, proximal bone loss can be minimized by optimizing proximal femoral stress distribution. Many designs have been made to improve proximal femoral stress distribution for cementless femoral stems. Until now, no certain design has been shown superior to others. Finite element analysis has been successfully used in orthopedic biomechanical studies.⁶ In this study, we compared 4 designs by calculation of the initial periprosthetic von Mises stress distribution by finite element analysis. Four proximal femoral replacement models were set up with stems of different contours. We aimed to reveal whether the contour of the stem is correlated with initial periprosthetic stress distribution.

Methods. The study was carried out at the Department of Orthopaedics, Shanghai 6th Hospital, Shanghai, China between May 2008 and February 2009. The ethics committee believed this research is only computer simulation study, and therefore ethics approval was not necessary. Four proximal femoral replacement digital models were created with a Chinese human virtual femur and 4 different stems. The loads applied were simulations of walking and stair climbing. Four currently used femoral stems were recruited: 1) Alloclassic SL (Zweymüller, Plus, Davos, Switzerland) with rectangular cross sections and vertical double-taper. 2) Ribbed Anatomic with proximal anatomic bows and ribs (Waldemar Link GmbH & Co, Hamburg, Germany). 3) VerSys Fiber Metal Taper with rounded corners and vertical tapered (Zimmer, Warsaw, USA). 4) Securi-fit with proximal blunt angle edges and double-wedge (Stryker, Kalamazoo, USA). The digital left femur was derived from a Chinese virtual human project, extracted from a 35-year-old, 65 kg male. A finite element model was created by using eight-node hexahedron isometric elements. Finite element models of 4 femoral stems were established. Proximal femoral replacement was simulated with the 4 stems. To eliminate interference, all the materials were assumed to be isotropic and linear elastic and cancellous bone is neglected. The elastic modulus of titanium alloy was set to 111.0 GPa, and cortical bone was set to 15.50 GPa. The Poisson's ratio of titanium alloy was 0.30 and cortical bone was 0.29.⁷ Distal femoral osteotomy was simulated and the distal end of the femoral model was fixed. Face

to face frictional contact models were simulated. The coefficient of friction was 0.4, and shrinkage limit (SL, describes the non-linear friction characteristics of the interface) was 0.1. The interface interference fit was 50 μm (Figure 1).⁸ The loading conditions were induced by the method from the report of Heller.⁹ The magnitude of each component was calculated based on the weight of the donor (Table 1). Two load conditions were applied to each model: walking and stair climbing. Finite element analysis was run by Abaqus 6.7-1 (Simulia, Shanghai Jiaotong University, China). The hardware of the computer included CPU: Dual Intel Pentium (R) CPU 3.00GHz; Memory: 2.00GB of RAM; Video card: NVIDIA Geforce 6600; Mainboard: Gigabyte 82915P; Monitor: SAMSUNG SyncMaster 997MB Plus. The average values of 3 dimensional stress distributions were calculated in the relevant zones according to Gruen's methods.¹⁰

Results. To clarify the patterns of 3 dimensional stress distribution, Gruen zones were further divided into 4 zones in each segment (anterior, lateral, medial, and posterior) with the method introduced by Jonkers et al.⁶ Periprosthetic von Mises stresses in each zone were calculated when the loading conditions were applied to the models. The results are shown in Figures 2 & 3. Compared with preoperative patterns, stresses were mainly increased in level 2, and 3. Von Mises stresses were also increased in level 1, but not at the considerable magnitude in level 2 and 3. In level 4, von Mises stresses were not changed significantly. Although

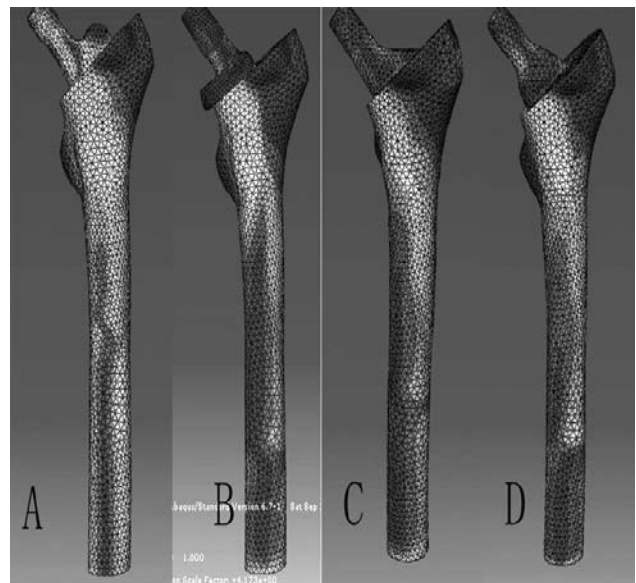


Figure 1 - The 4 finite element models used in this simulation. (A - Alloclassic, B - Ribbed, C - VerSys, and D - Securi-fit)

Table 1 - The stair climbing loading conditions.

Forces (N)	walking			Stair climbing		
	x	y	z	x	y	z
Hip contact	-343.98	-208.936	-1460	-377.741	-386.022	-1505.23
Abductor	369.46	27.391	551.005	446.537	183.456	540.813
Tensor fascia latae, proximal part	45.864	73.892	84.084	19.747	31.213	18.473
Tensor fascia latae, distal part	-3.185	-4.459	121.03	-1.274	-1.911	-41.405
Iliotibial tract, proximal part				66.885	-19.11	81.536
Iliotibial tract, distal part				-3.185	-5.096	-107.016
Vastus lateralis	-5.733	117.845	-591.773	-14.014	142.688	-860.587
Vastus medialis				-56.056	252.252	-1701.43

the patterns of von Mises stresses distribution changed after arthroplasty, similar patterns of the average von Mises stresses distribution in 3D zones were found in the 4 models with different stems. The highest stress was found in the medial side in all cases. Between the 2 loading conditions, the von Mises stresses were different only in magnitude, and the trends remained the same. No significant different of stress distribution pattern was found between the 4 models.

Discussion. Periprosthetic bone loss is a major concern with hip arthroplasty. Bone is sensitive to mechanical stimuli. Many investigations have been performed to evaluate periprosthetic stress distribution. The major studies on periprosthetic stress distribution of cementless femoral stem set the interfacial condition as bonded, while ignoring the effect of press-fit.⁶ Although the stress relaxation effect is significant following press-fit implantation, the pressure between the prosthesis and bone continues in certain degrees, which is essential to maintain the primary stability of the prosthesis before osseointegration is completed. It has been demonstrated that major bone loss occurs several months postoperatively, and bone stock maintains stable thereafter.^{4,5} To improve the longevity of arthroplasty, many kinds of designs have been developed. The optimal contour for the femoral stem is not known. It seems that most of the stems being used provide similar results.¹¹⁻¹⁴

In this study, we used the press-fit femoral replacement models to calculate periprosthetic von Mises stresses distribution. We found that von Mises stresses were increased in Level 1, 2, and 3. The patterns of stress distribution were similar in the 4 models created with variant stem contours. We did not carry out statistical analysis for the results in this study, because we believe

the magnitude of difference is not significant clinically.

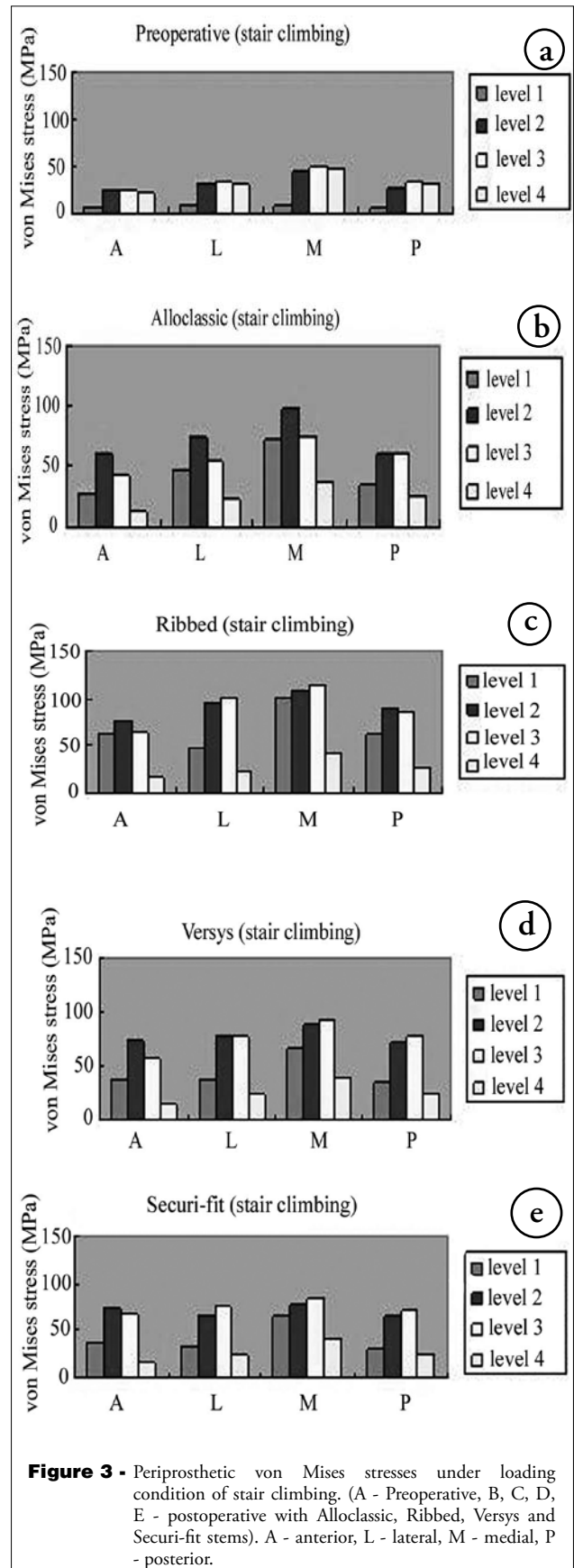
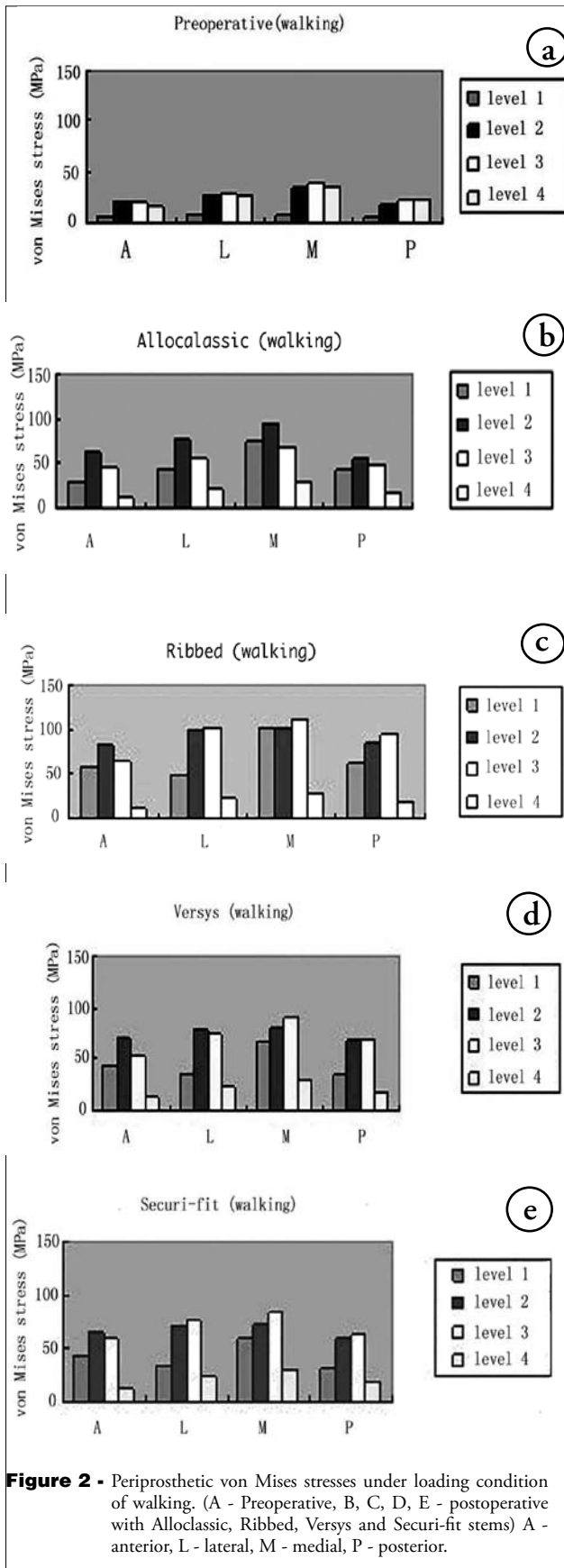
It could be argued that the increased stress is contradictory to the significant bone loss after arthroplasty. We think this can be contributed to nonphysical stresses (direction and magnitude). Press-fit fixation and loading on the prosthesis lead to high transverse pressure, which ends in increased periprosthetic von Mises stresses. This transverse high pressure is not physical stress. The biologic reaction to this stress may be different. Transverse pressure was used to induce osteolysis in orthodontic practices.¹⁵ In an animal study, press-fit has been demonstrated to induce periprosthetic bone absorption, which can be improved by Alendronate.¹⁶

Recently, Stiehl¹⁷ demonstrated that major bone loss after cementless hip arthroplasty occurred in Gruen zones 1, 2, 6, and 7. However, when compared with the contralateral unaffected femur, major bone loss only occurred in Gruen 7 zone, and bone stock was maintained in 3, 4, and 5 zones of the proximal femur.

The 4 femoral stems have been widely used clinically. However, one has not been found superior to the others. Our study results revealed that the patterns of stress distribution are similar with the 4 stems, which may explain the clinical results.

This study focused on initial periprosthetic stress distribution. In the long term following arthroplasty, because of stress relaxation, and osseointegration, the mechanical environment would be different. To evaluate the different design of femoral stems, further study is needed to compare the long-term periprosthetic stress distribution. The limitation of this finite element model is that cancellous bone was neglected to simplify simulation. To further understand the periprosthetic stress distribution, more details should be investigated.

In conclusion, the contour design of the femoral stem has minor effect on initial periprosthetic von Mises



stress distribution. The characteristic of periprosthetic stress should be considered when analyzing the effect of periprosthetic stresses.

References

1. Bodén H, Salemyr M, Sköldenberg O, Ahl T, Adolphson P. Total hip arthroplasty with an uncemented hydroxyapatite-coated tapered titanium stem: results at a minimum of 10 years' follow-up in 104 hips. *J Orthop Sci* 2006; 11: 175-179.
2. Kaya M, Nagoya S, Sasaki M, Kukita Y, Yamashita T. Primary total hip arthroplasty with Asian-type AML total hip prosthesis: follow-up for more than 10 years. *J Orthop Sci* 2008; 13: 324-327.
3. Morscher EW. Failures and successes in total hip replacement--why good ideas may not work. *Scand J Surg* 2003; 92: 113-120.
4. Aldinger PR, Sabo D, Pritsch M, Thomsen M, Mau H, Ewerbeck V, et al. Pattern of periprosthetic bone remodeling around stable uncemented tapered hip stems: a prospective 84-month follow-up study and a median 156-month cross-sectional study with DXA. *Calcif Tissue Int* 2003; 73: 115-121.
5. Venesmaa PK, Kröger HP, Miettinen HJ, Jurvelin JS, Suomalainen OT, Alhava EM. Monitoring of periprosthetic BMD after uncemented total hip arthroplasty with dual-energy X-ray absorptiometry--a 3-year follow-up study. *J Bone Miner Res* 2001; 16: 1056-1061.
6. Jonkers I, Sauwen N, Lenaerts G, Mulier M, Van der Perre G, Jaecques S. Relation between subject-specific hip joint loading, stress distribution in the proximal femur and bone mineral density changes after total hip replacement. *J Biomech* 2008; 41: 3405-3413.
7. Sakai R, Kanai N, Itoman M, Mabuchi K. Assessment of the fixation stiffness of some femoral stems of different designs. *Clin Biomech* 2006; 21: 370-378.
8. Abdul-Kadir MR, Hansen U, Klabunde R, Lucas D, Amis A. Finite element modelling of primary hip stem stability: the effect of interference fit. *J Biomech* 2008; 41: 587-594.
9. Heller MO, Bergmann G, Kassi JP, Claes L, Haas NP, Duda GN. Determination of muscle loading at the hip joint for use in pre-clinical testing. *J Biomech* 2005; 38: 1155-1163.
10. Gruen TA, McNeice GM, Amstutz HC. "Modes of failure" of cemented stem-type femoral components: a radiographic analysis of loosening. *Clin Orthop Relat Res* 1979; 17-27.
11. Fortina M, Carta S, Gambera D, Crainz E, Pichierrri P, Ferrata P. Total hip arthroplasty with a ribbed anatomic HA coated stem. *J Orthopaed Traumatol* 2006; 7: 122-125.
12. Marshall DA, Mokris GJ, Reitman DR, Dandar A, Mauerhan DR. Cementless titanium tapered-wedge femoral stem: 10- to 15-year follow-up. *J Arthroplasty* 2004; 19: 546-552.
13. Incavo SJ, Beynnon BD, Coughlin KM. Total hip arthroplasty with the Secur-Fit and Secur-Fit plus femoral stem design: a brief follow-up report at 5 to 10 years. *J Arthroplasty* 2008; 23: 670-676.
14. Nishino T, Mishima H, Miyakawa S, Kawamura H, Ochiai N. Midterm results of the Synergy cementless tapered stem: stress shielding and bone quality. *J Orthop Sci* 2008; 13: 498-503.
15. Masella RS, Meister M. Current concepts in the biology of orthodontic tooth movement. *Am J Orthod Dentofacial Orthop* 2006; 129: 458-468.
16. Jensen TB, Bechtold JE, Chen X, Søballe K. Systemic alendronate treatment improves fixation of press-fit implants: a canine study using nonloaded implants. *J Orthop Res* 2007; 25: 772-778.
17. Stiehl JB. Long-term Periprosthetic Remodeling in THA Shows Structural Preservation. *Clin Orthop Relat Res* 2009. [Epub ahead of print].

Related topics

Zamzam MM. Congenital osteofibrous dysplasia of the tibia, associated with pseudoarthrosis of the ipsilateral fibula. *Saudi Med J* 2008; 29: 1507-1509.

Uzel M, Ergun GU, Ekerbicer HC. The knowledge and attitudes of the primary care physicians on developmental dysplasia of the hip. *Saudi Med J* 2007; 28: 1430-1434.

Moussa M, Alomran A. Acetabular dysplasia in adult hips of a Saudi population. A possible relation to coxarthrosis. *Saudi Med J* 2007; 28: 1059-1061.

Unal VS, Gulcek M, Soydan Z, Ucaner A, Yazici M. Assessment of quality of life in children after successful treatment of hip dysplasia as compared with normal controls. *Saudi Med J* 2006; 27: 1212-1216.